

Determination of the Bending Characteristic Parameters of the Bending Evaluation System of Fabric and Yarn

Abstract The bending evaluation system of fabric and yarn (BES-FY) can measure the bending, weight, friction and tensile properties of fabric and yarn through a pull-out test and delineate the relationship between the mechanical geometry and the corresponding deforming process, so as to quantify the comprehensive hand of fabric and yarn. The bending process of the BES-FY system was mainly investigated in the present study. Two bending models were developed under different conditions and the corresponding formulae for bending rigidity were also obtained. The optimum point and range for calculating the bending rigidity was acquired by experimental and analytical investigation, which involved study of the relationships between bending rigidity–curvature. These can be divided into three sections, namely, linear, quadratic and constant function, and through the comparisons between the bending rigidity of the two bending models and that of KES-FB2 and FAST-2, the better bending model was selected to characterize the bending properties of fabric and yarn.

Key words bending rigidity, yarn, fabric, three point bending, handle system

Weidong Yu^{1,2} and Zhaoqun Du

*College of Textiles, Dong Hua University,
Shanghai 200051, People's Republic of China*

The bending behavior of fabric and yarn plays an important role in the handling properties and the end-use performance of textiles. So, many authors have been studying the handle of fabric or even yarn by measurements of mechanical properties, especially for the bending property [1–5]. Some useful apparatus and instruments have been developed for the measurements, in which the most commonly and commercially used equipments are Kawabata's evaluation system for fabrics (KES-F) system [6] and the fabric assurance by simple testing (FAST) system [7].

The two systems, however, both include four parts and are just used for characterization of the handle of fabric, but not for bending measurements on yarn. It is obvious that the KES-FB2 bending meter is not suitable for yarn because it is based principally on the pure horizontal bending, whereas the FAST-2 bending meter is based on canti-

lever bending which easily results in deviations from the effect of the free end of the yarn [8, 9].

Therefore, a patented and applicable apparatus [10, 11] has been designed and developed by the authors to measure the bending, weight, friction and tensile properties for both fabric and yarn in-situ by a pull-out test. The bending principal of the apparatus based on a quasi-tri-point bending can make up for the deficiency of the KES-FB2 and FAST-2, and can also be used in other measurements. Based mainly on the apparatus, we constructed a bending model to establish the equations of the bending rigidity and to obtain the

¹ Corresponding author: e-mail: wdyu@dhu.edu.cn

² Also at Wuhan University of Science and Engineering, Wuhan 430073, People's Republic of China.

characteristic stages and parameters in a pull-out test of a fabric or a yarn.

Analytical Model

The fundamental structure of BES-FY is illustrated in Figure 1 which is a quasi three point bending device combining a fixed pin with two U-shaped pins. A yarn or a fabric is clamped and hung on the two jaws and is bent between the fixed pin and the two U-shaped pins. If the yarn/fabric has no extension; then the cross-section of the yarn/fabric does not change in the whole bending; the bending between the fixed pin and the U-shaped pins follows Timoshenko's elastic theory [12]; and there exists only a small deformation in the bending of the yarn/fabric in the initial period.

The U-shaped pins with the sample are of circular cross-section. For modeling conveniently, however, it was assumed that one is circular in cross-section for shifting-point bending (fabric slides over the pin), and the other is semicircular for fixed-point bending (no sliding). The two bending models based on the BES-FY are illustrated in Figure 2 and were analysed in the following manner.

The contacting part of the fixed pin is at the center point of the sample length between the U-shaped pins. The

maximum deflection, x , of the sample is increased by the pulling up of the U-shaped pins. The assumed arc length, $l(x)$, of the center line of the sample between the U-shaped

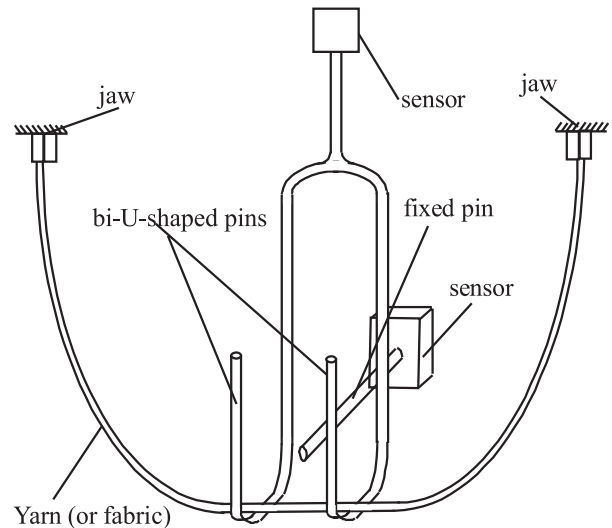


Figure 1 The fundamental structure of BES-FY.

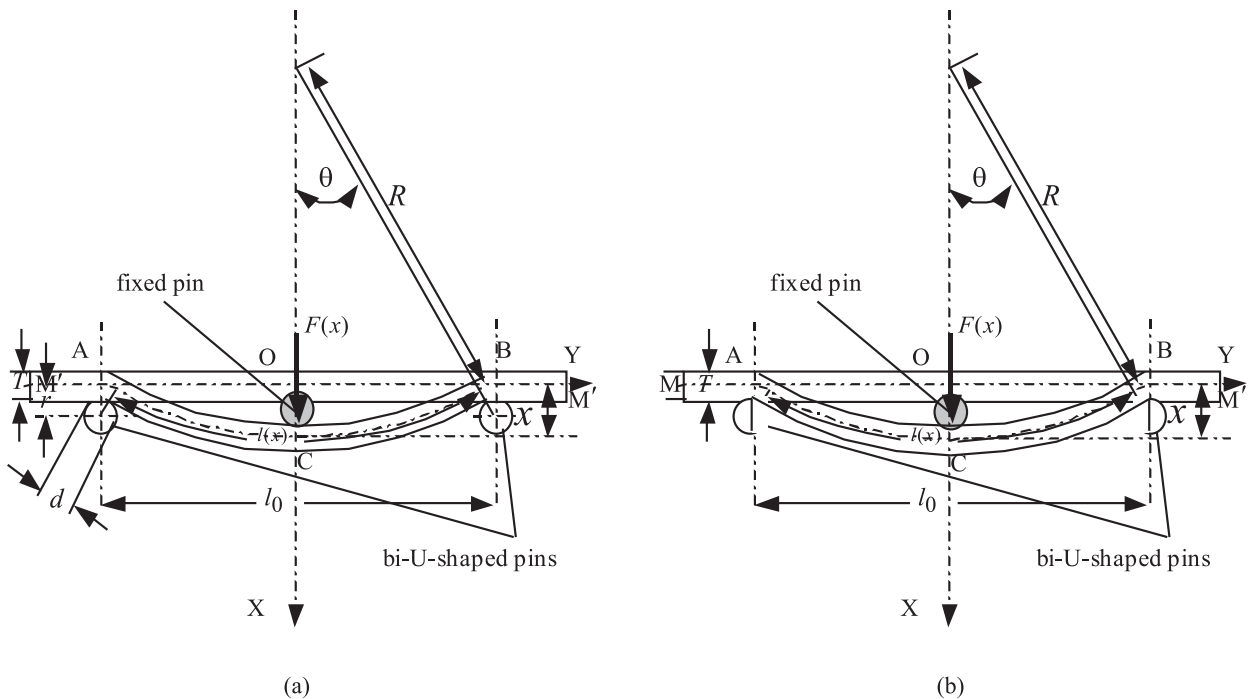


Figure 2 The fundamental principals of two bending models for the BES-FY system. (a) Bending model for the shifting point. (b) Bending model for the fixed point.

pins and the reaction force, $F(x)$, on the fixed pin are both changed with the pulling shift, i.e., the length and the reaction force are functions of maximum deflection. Therefore, by designating the center line vertical to the sample in the horizontal linear status as the X -axis and the horizontal linear sample as the Y -axis to be the Cartesian coordinates of the structure, the bending formula is as follows:

$$x = F(x) \cdot l^3(x)/(48B), \tag{1}$$

$$l(x) = 2R\theta. \tag{2}$$

Bending Modeling for Shifting Point

The shifting-point bending model (SBM) is considered in which the contacting point between the sample and the U-shaped pins is gradually changing along the circular contour, so, according to Figure 2a, R and θ can be expressed as

$$R\sin\theta + r\sin\theta = l_0/2,$$

$$R - (R + r)\cos\theta = x - r,$$

thus

$$R = [l_0^2/4 + x^2 - 2rx]/(2x), \tag{3}$$

$$\theta = \arcsin[(l_0x)/(l_0^2/4 + x^2)], \tag{4}$$

where $r = (d + T)/2$; d is the diameter of the U-shaped pins and T is the sample thickness.

By substituting equations (3) and (4) into equation (2), we get

$$l(x) = \left(\frac{l_0^2/4 + x^2 - 2rx}{x}\right) \cdot \arcsin[l_0x/(l_0^2/4 + x^2)]. \tag{5}$$

From equation (5) and equation (1), the bending rigidity, B , can be found

$$B \cdot x = F(x) \left[\left(\frac{l_0^2/4 + x^2 - 2rx}{x}\right) \cdot \arcsin(l_0x/(l_0^2/4 + x^2)) \right]^3 / 48 \tag{6}$$

On differentiating equation (6) with respect to the maximum deflection, x , we find

$$\frac{3B = F'(x)[R\theta]^4}{8x^3R\theta - 3x^4[(1 - l_0^2/(4x^2))\theta + 2l_0R(l_0^2/4 - x^2)/(l_0^2/4 + x^2)^2 \cos\theta]} \tag{7}$$

Bending Modeling for Fixed Point

The fixed-point bending model for the semicircular cross-section (FBM) is considered in which the contacting point between the sample and the U-shaped pins is invariable and stays at the highest point of the semicircular cross-section. So the bending is simplified into the bending of the simply supported beam, and from Figure 2b, R and θ can be found as

$$\left(R + \frac{T}{2}\right)^2 = \left(\frac{l_0}{2}\right)^2 + \left(R + \frac{T}{2} - x\right)^2,$$

$$\sin\theta = \frac{l_0}{2(R + T/2)}.$$

So that

$$R = (l_0^2/4 + x^2 - Tx)/2x, \tag{8}$$

$$\theta = \arcsin\frac{l_0x}{l_0^2/4 + x^2}. \tag{9}$$

Substituting equation (8) and equation (9) into equation (2), we get

$$l(x) = 2R\theta = \left(\frac{l_0^2/4 + x^2 - Tx}{x}\right) \cdot \arcsin\left(\frac{l_0x}{l_0^2/4 + x^2}\right). \tag{10}$$

From equation (10) and equation (1), We found

$$B \cdot x = F(x) \cdot \left[\left(\frac{l_0^2/4 + x^2 - Tx}{x}\right) \cdot \arcsin\left(\frac{l_0x}{l_0^2/4 + x^2}\right) \right]^3 / 48. \tag{11}$$

By differentiating equation (11) with respect to x , it can be obtained

$$\frac{3B = F'(x) \cdot [R\theta]^4}{8x^3R\theta - 3x^4[(1 - l_0^2/(4x^2))\theta + 2l_0(l_0^2/4 - x^2)R/(l_0^2/4 + x^2)^2 \cos\theta]} \tag{12}$$

In fact, according to the model FBM, there exist the tension and elongation in the bending sample, and the extension, ϵ_{FRW} , of the sample is equal to $(l(x) - l_0)/l_0$, i.e.,

$$\epsilon_{FBM} = \frac{2R\theta}{l_0} - 1. \tag{13}$$

Therefore, the reaction force of the fixed pin in equation (1) should be modified into $(F(x) + E\epsilon_{FBM})$, where E is tensile modulus, but equation (1) is still viable because

the low-tension action can be negligible under the small deformation.

The bending rigidity, however, is actually variable and is a nonlinear function of the curvature and the maximum deflection. Consequently, the differentiation of bending rigidity with respect to the maximum deflection in equation (6) and (11) is not constant, which will cause complications in calculating the bending rigidity of a fabric or a yarn. Therefore, bending rigidity is assumed to be a constant, and the validity of the assumption is checked for the large curvature condition from the following experiments.

It can be found from the comparison of the above two bending models that the equations for the force action angle, θ , is the same, whereas the equations for the radius of curvature, R , are different in r and T , because $2r > T$, the bending rigidity, B , obtained from equation (6) is lower than that from equation (11) in theory.

By measuring $F(x)$ and x , the bending rigidity of a fabric or a yarn can be obtained through equation (6) or (7) (for the SBM) and equation (11) or (12) (for the FBM), respectively. The bending rigidity for fabric per unit width is equal to the bending rigidity divided by the width of the measured fabric, which is conveniently used to have a comparison between the measured results and that of KES-FB2 and FAST-2.

Experimental

Materials and Methods

All the wool/polyester yarns, and fabrics woven from these yarns with the warp \times weft gauge length of 15 cm were selected from a Shanghai wool textile mill, and all the samples were conditioned in $(20 \pm 2)^\circ\text{C}$, $(65 \pm 3) \% \text{RH}$ for about 24 hours before the testing.

Then, the parameters of the BES-FY instruments were set as follows, the diameters of the fixed pin and the U-shaped pins were 0.6 mm; the distances of the U-shaped pins and the two jaws were 8 mm and 5 cm, respectively; the vertical distance from the hanging point of the jaw to

the fixed pin was 6 cm; the speed of upward movement of the U-shaped pins was 6 mm/min; and the sampling frequency of the A/D Convectator was 100 Hz.

Finally, the experiments of the yarns and fabrics tested by KES-FB2, FAST-2 and BES-FY, respectively, were carried out under the standard condition defined above. The bending rigidity of yarn, B_Y , was calculated from the corresponding bending rigidity of the fabric, B_F by the following equation, and vice versa [13].

$$B_Y = B_F \cdot (1 + C) \cdot 10/D. \quad (14)$$

All the known parameters and the specification of these samples are listed in Table 1.

In Table 1, BR is the blend ratio of Wool/PET yarn; T is the thickness of fabric; N_A is the linear density of warp Wool/PET yarn measured by weight method; G_A is the weight per square meter of the fabric; D is the pick count of fabric per 10 cm; B_{F2} and B_{F3} are the bending rigidity of fabrics measured by KES-FB2 and FAST-2, respectively; B_{Y2} and B_{Y3} are calculated from B_{F2} and B_{F3} through equation (14), respectively; where C is the warp yarn crimp calculated by the equation:

$$C = (C_1 - C_0)/C_0, \quad (15)$$

where C_1 and C_0 are the length of yarn and the length of fabric, respectively, in the unit repetition of weave.

Typical Reaction Force – Maximum Deflection Curve

The typical bending procedure of a yarn or a fabric by using the BES-FY is shown in Figure 3a, and the smoothed (with a filter) 11-point Savitzky–Golay curve, corresponding to each step of the sample deformation in Figure 3a, is illustrated in Figure 3b.

According to the mechanism of the deformation in this measuring system, the testing procedure can be divided into five steps.

Table 1 The specification of wool/PET fabrics.

No.	BR	T (mm)	N_A (tex)	G_A (g/m ²)	D (10cm)	B_{F2} (cN · cm)	B_{Y2} (cN · cm ²)	B_{F3} (cN · cm)	B_{Y3} (cN · cm ²)	C (%)
1	45/55	0.328	28.1	226	320	0.164	0.00562	0.202	0.00691	9.5
2	60/40	0.434	27.7	261	441	0.227	0.00559	0.257	0.00631	8.5
3	50/50	0.426	34.5	272	320	0.2045	0.00692	0.242	0.00816	8
4	70/30	0.472	28.2	287	444	0.234	0.00568	0.267	0.00647	7.5
5	65/35	0.438	24.1	242	592	0.267	0.00480	0.329	0.00591	6.5
6	80/20	0.302	26.9	189	289	0.152	0.00562	0.167	0.00618	7.0
7	90/10	0.388	27.2	259	483	0.240	0.00525	0.285	0.00625	6.0
8	100	0.514	32.9	294	371	0.188	0.00534	0.240	0.00683	5.5

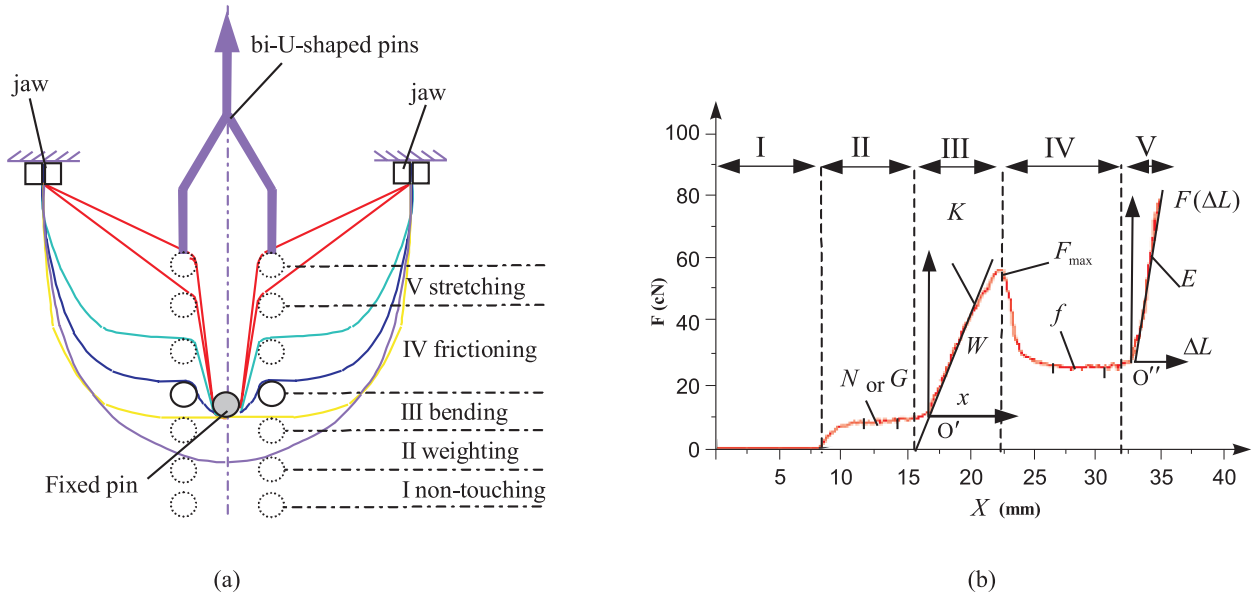


Figure 3 The principal schematic diagrams for each step of the one pulling-out measurement. (a) A tri-point bending process. (b) The typical reaction force–maximum deflection curve.

The first step is non-touching movement of the U-shaped pins, that is the “I” region that can be used as the calibration for force zero point.

The second step is the movement of the U-shaped pins touching the sample, but not touching the fixed pin, thus the dominant action of the step, “II”, is the sample weighting step. The linear density of yarn (N) and the weight per square meter of fabric (G) can be found from this data.

Step “III” is the bending region because the sample begins bending due to the actions of both the U-shaped pins and the fixed pin so that the line with the maximum bending slope (K) can easily be drawn. The bending range of III is defined as the range from three points touching the sample to the maximum bending force (F_{max}). Geometrically, the step begins at point, O' , which is the point of intersection of the line with tangent K and axis x . The

bending work (W) can be integrated from the curve in step III.

When the bending force reaches a maximum, the sample slides over the U-shaped pins overcoming friction, the characteristic parameter is the sliding friction force (f), and the step is called as “IV”. Step IV is a friction (fabric or yarn) step, and stops at the sample stretching.

If the sample begins stretching, it is called stretching step “V”, so that the tensile modulus (E) can be derived from the tangent with the maximum slope.

The force, $F(x)$, in a whole deformation is recorded with the shift, X , of the bi-U-shaped pins as shown in Figure 3(b). For the analysis of bending rigidity, only the region of step III is considered that the initial point changes to the bending beginning point (O'), thus the force–shift curve represents $F(x)$ – x . Similarly, for the tensile step, the initial point

Table 2 Measured results of the wool/PET yarns and fabrics by BES-FY.

No.	N_B (tex)	G_B (g/m ²)	B_{Y1} (SBM) (cN · cm ²)	B_{Y1} (FBM) (cN · cm ²)	B_{F1} (SBM) (cN · cm)	B_{F1} (FBM) (cN · cm)	f_Y (cN)	F_F (cN)	E_Y (cN/tex)	E_F (cN/cm)
1	27.9	229	0.00660	0.00683	0.2020	0.2081	1.932	15.917	0.1038	24.665
2	27.5	264	0.00596	0.00613	0.2528	0.2560	2.983	16.189	0.1138	27.684
3	34.8	272	0.00791	0.00802	0.2420	0.2470	3.224	15.634	0.1224	24.413
4	28.2	280	0.00609	0.00623	0.2618	0.2731	3.356	16.703	0.2108	29.013
5	23.7	246	0.00519	0.00548	0.2980	0.2980	2.327	15.010	0.0974	25.663
6	26.7	192	0.00565	0.00582	0.1563	0.1611	2.847	21.657	0.0894	23.684
7	27.0	261	0.00571	0.00593	0.2677	0.2711	3.130	30.755	0.2093	35.923
8	32.7	291	0.00634	0.00657	0.2300	0.2483	2.714	22.201	0.1629	28.321

is O'' , and the relationship is $F(\Delta L)-L$. The characteristic of each step is clear for the one pulling-out test by the quasi-tri-point apparatus. Therefore, it is evident that each characteristic parameter, i.e., weight, bending, friction and tensile properties of the yarns or fabrics, can be evaluated by means of the force-shift curve. In this paper, the subscripts, Y and F, for all the symbols are used as the results of yarn and fabric, respectively, and the subscripts next, 1, 2 and 3, represent the measurement of BES-FY, KES-FB2, FAST-2 respectively, e.g. as shown in Tables 1 and 2.

In Table 2, N_B , B_{Y1} , f_Y and E_Y are the linear density, bending rigidity, average frictional force and tensile modulus of yarn measured by BES-FY, respectively; and G_B , B_{F1} , f_F and E_F are the weight per square meter, bending rigidity, average frictional force and tensile module of the fabrics measured by BES-FY, respectively.

Results and Discussion

The Effects of Sample Parameters on the Bending Rigidity

Figures 4–7 show the typical relationships between bending rigidity and maximum deflection, The bending rigidity–ratio of maximum deflection to the distance of the bi-U-shaped pins, bending rigidity–extension of the sample, and bending rigidity–curvature curve, which was calculated on the basis of the force-shift curve given in Figure 3b and the theoretical formulas of the two bending models (i.e., equations (6) or (7), and equations (11) or (12), respectively).

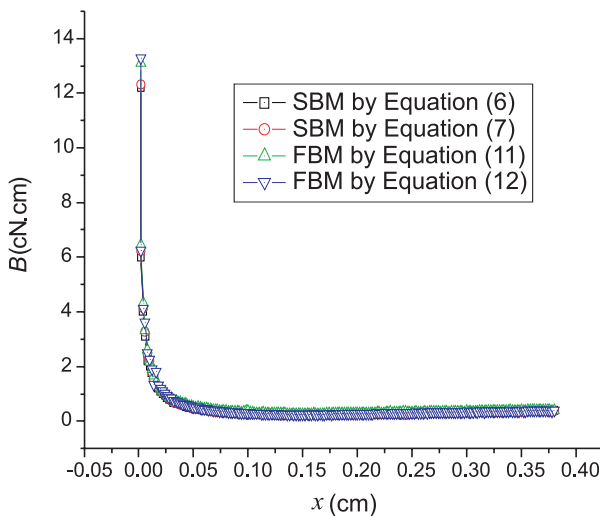


Figure 4 Bending rigidity – maximum deflection curve.

It can be seen from Figures 4–7 that the bending rigidity decreases nonlinearly with the increase of the maximum deflection, x , the ratio of the maximum deflection x to the distance l_0 of the U-shaped pins, the extension ϵ [i.e., $(l(x) - l_0)/l_0 \times 100\%$] of the sample length between U-shaped pins and the curvature and all the curves have the same shape. The variations of bending rigidity calculated by equations (6) and (7) and equations (11) and (12) are both not larger than 0.022 and can be regarded as approximately equal and

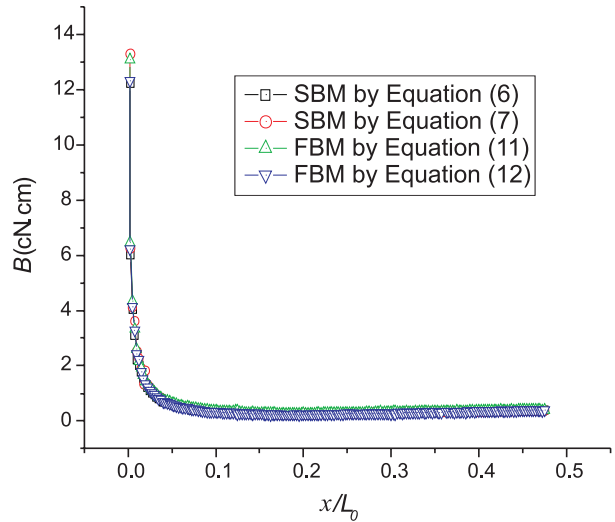


Figure 5 Bending rigidity – ratio of maximum deflection to the distance of the bi-U-shaped pins curve.

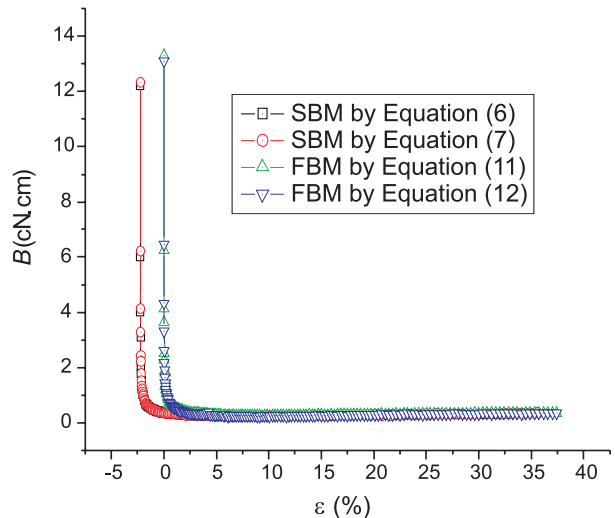


Figure 6 Bending rigidity – the extension of the sample length of the bi-U-shaped pins curve.

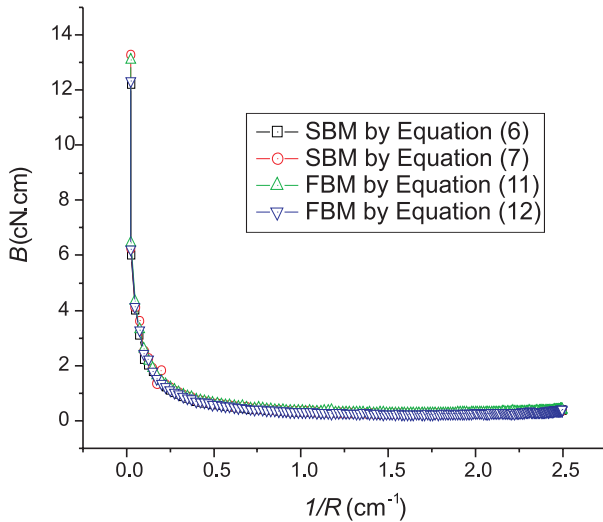


Figure 7 Bending rigidity – curvature curve.

will be further discussed, whereas the deviation of the bending rigidity from the two bending models is higher (0.08). Therefore, the bending rigidity of a fabric or a yarn can be calculated by equations (6) and (11) (see Table 2) because of the complicated nature of equations (7) and (12).

In the early part of these curves, the bending rigidity, B , is high but rapidly decreases linearly in the initial region, which implies a high initial resistance to bending, probably because of the need to work to overcome the frictional resistances at fiber/fiber contact points in the yarn and at yarn/yarn contact areas in the fabric. These frictional forces, set up a couple that opposes bending, often referred to as the frictional or coercive couple [14]. By fitting the part of the curve of the bending rigidity and curvature in that region, the correlation coefficient obtained reached 0.878. The linear relationship between the bending rigidity, B , and curvature, $1/R$, implies a quadratic relationship between the bending moment and curvature, which is the same as Abbott *et al.*'s bending model [15].

In the following region, the bending rigidity is gradually falling, which may be explained as the yarn cross-section area is slowly reducing because of the weak inter-compressing deformation of warp and weft yarns, which causes a decrease of the cross-section inertial moment of fabric. By fitting the section of the curve of the bending rigidity and curvature in the region to a quadratic, the correlation coefficient reached 0.985. The linear relationship between the bending rigidity and curvature indicates a polynomial function of order three for the bending moment and curvature, which is similar to Clapp *et al.*'s model [16] that tries to use a cubic-spline-interpolation method to express the measured moment–curvature relationships. The precision

is high in quantifying the bending rigidity, but the definite numbers of the regions in the measured moment–curvature curve is not given and difficult to be divided.

Finally, the bending rigidity B tends towards a constant value in the final region as shown in Figures 4–7. After the frictional restraint has been overcome and the inter-compressing deformation of warp and weft yarns has become very small, the fibers in the yarn and yarns in the fabric only slip over each other with great difficulty or not at all. By analyzing the constant bending rigidity, the standard deviation and the coefficient of variation were 0.00645 and 0.025. The invariable nature of the bending rigidity with curvature implies a linear function of the bending moment and curvature, which can be proved by a number of models [17–19]; the relationships of moment–curvature are usually divided into two regions, and the last region is linear in these models.

Recently, Kang *et al.* [20] fitted the whole moment–curvature curve measured by KES-FB2 to an exponential function, through the exponential model, so that the bending rigidity was easily calculated at any curvature value. However, a highly accurate value for the bending rigidity could not be obtained and the exponential function was inadequate to meet different stages' of the study of moment–curvature relationship (see Figures 4–7).

Based on the above discussion and the bending rigidity–curvature plot, we suggest that the moment–curvature relationships may be divided into three sections, the first section is quadratic, the second section is a polynomial of order three and the last section is linear. The corresponding curvature ranges for the three sections are 0–0.2 cm^{-1} , 0.2–1.5 cm^{-1} and 1.5–2.5 cm^{-1} . Although the curvature ranges for the three sections are fitted just by Wool/PET yarns and fabrics, these results are very typical and will be further verified by measurements on several fabrics woven from different kinds of fibers.

The Effect of Instrument Parameters on the Bending Rigidity

The effects of parameters of the BES-FY apparatus, such as the distance between the U-shaped pins, the sample length mounted on the two jaws, the diameter and the speed of upward motion of the U-shaped pins on the bending rigidity calculated at the curvature 1.5 cm^{-1} are illustrated in Figures 8–11, respectively.

The results in Figure 8 indicate that the bending rigidity presents a slowly descending trend as the distance between the U-shaped pins increased from 4 to 20 mm, but the bending rigidity can be regarded as invariable when the distance of the U-shaped pins was 5 to 14 mm. The standard deviation and the coefficient of variation were 0.000134 and 0.00564 for 5–14 mm, respectively. In general, the geometrical irregularity of the sample length in the bending step increases with the increasing distance between the U-shaped

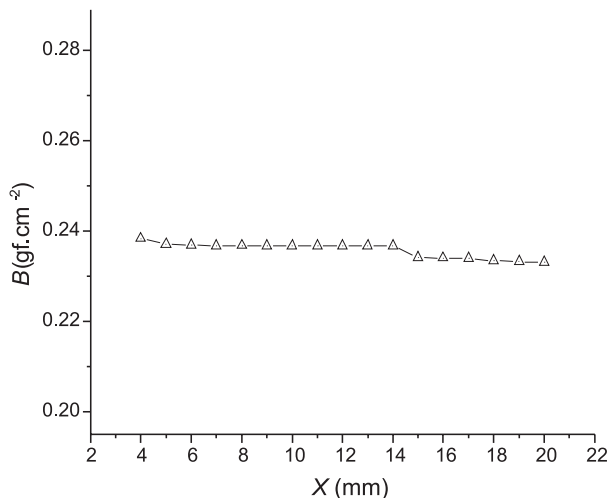


Figure 8 Bending rigidity - U-shaped pins distance curve.

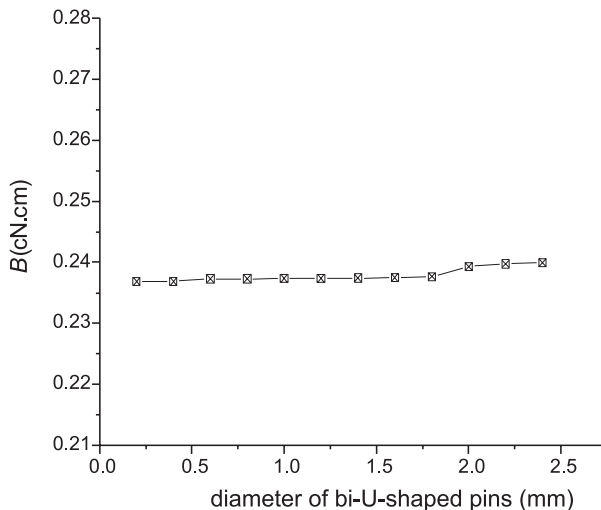


Figure 10 Bending rigidity - diameter of U-shaped pins curve.

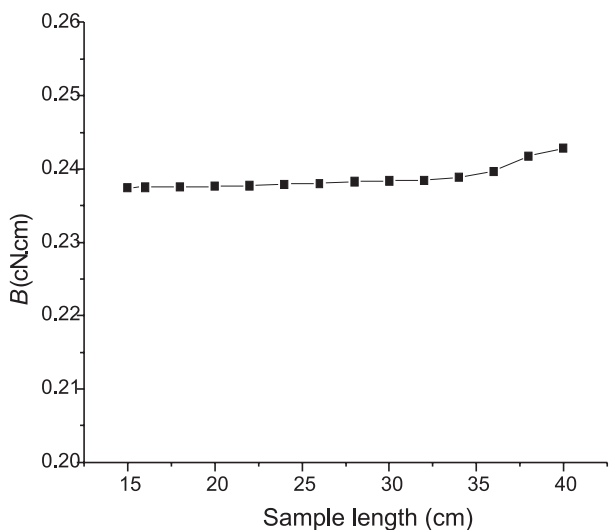


Figure 9 Bending rigidity - sample length curve.

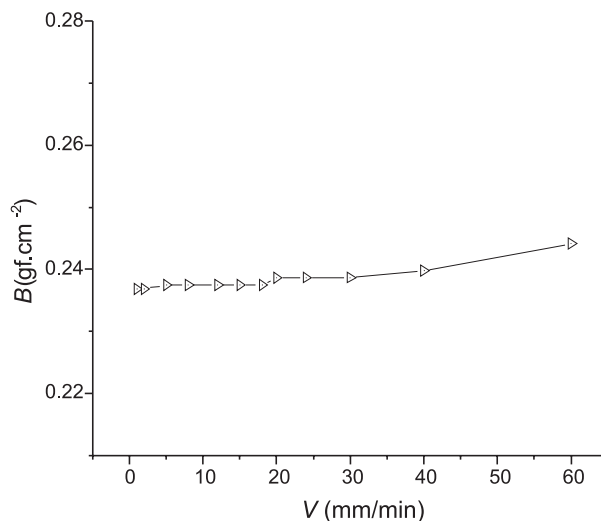


Figure 11 Bending rigidity - U-shaped pins speed curve.

pins. However, when the distance of the U-shaped pins is gradually expanded, the length and weight of the sample hung between the jaw and the neighboring pin of the U-shaped pins is decreasing and therefore the effect of the frictional force between the U-shaped pins and the sample in terms of bending rigidity will also decrease.

Similarly, when the sample length is increased from 15 to 40 cm the frictional force between the U-shaped pins and the fabric or yarn will also increase. Because of this the bending rigidity shows a gradual increase, as shown in Figure 9, and the bending rigidity is also a constant when

the sample length is in the region of 15–24 cm, because the standard deviation and the coefficient of variation were 0.000173 and 0.000727, respectively in this range, which is acceptable. In addition, Figure 10 shows that the bending rigidity increases with the diameter of the bi-U-shaped pins, probably because the increase of the contacting angle [19] between the sample and the U-shaped pins enhances the force acting at the end point of the sample bending step, requiring a higher force to overcome bending.

Based on the study of the effect of the speed of upward movement of the U-shaped pins on the bending rigidity, we mainly want to discuss the effect of the bending rate [22] on the bending rigidity, when the speed of upward movement of the U-shaped pins ranges from 2 to 20 mm/min, compared to the static bending of the sample, because the different speeds, i.e., the bending rate is different. This is caused by an increase in fiber/fiber friction in yarn and yarn/yarn friction in the fabric as a function of speed, which requires a higher reaction force to overcome the coercive couple. Therefore, the bending rigidity calculated from the two bending models is variable. Generally, the higher the speed of upward movement of the U-shaped pins, the higher the bending rigidity, as shown in Figure 11. However, when the speed or the bending rate is very high, the bending test is like an impacting action on the sample; the effect of the bending rate on the bending rigidity needs to be further studied for such extreme conditions.

The Comparisons of Bending Rigidity Tested by BES-FY, KES-FB2 and FAST-2

In order to check the validation of the BES-FY system and determine the best bending model, the graphs and the correlations between the bending rigidity of the fabrics calculated from the corresponding bending rigidity of yarns measured by BES-FY through equation (14), the bending rigidity of the eight Wool/PET fabrics by BES-FY, KES-FB2 and FAST-2 are shown in Figure 12 and listed in Table 3.

From Figure 12, it can be concluded that there is good correlation between the three measurements in characterizing the bending rigidities of fabric, thereby verify that the two bending models are feasible in characterizing the bending rigidity of fabric and yarn, and the bending rigidity calculated from FBM is larger than that from SBM. The main reason is that the assumptions and the calculation for the two bending models are different and so the bending rigidity is different.

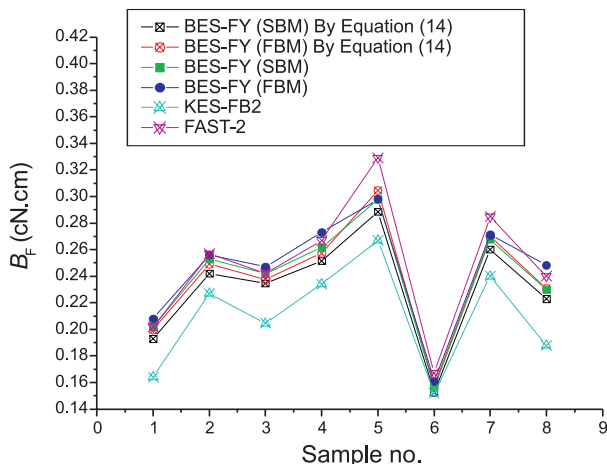


Figure 12 The bending rigidity of fabric by BES-FY, KES-FB2 and FAST-2.

From Table 3, the correlation coefficients between the bending rigidity of fabric calculated by theoretical equation for the two bending models, i.e., B_{F1} (SBM) and B_{F1} (FBM), with B_{F2} and B_{F3} are almost equal (see equations (6), (7), (11) and (12)), so both of the models are good in terms of the characterization of the bending rigidity of yarn. The correlation coefficients between B_{F1} (SBM) and B_{F2} or B_{F3} are more significant than that between B_{F1} (FBM) and B_{F2} , or B_{F3} . Therefore, the correlations between SBM and KES-FB2 or FAST-2 show that, in terms of characterizing the bending properties of fabric, the SBM is better. Moreover, the correlation coefficient between B_{F1} (SBM) and B_{F1} (SBM) by equation (14) is larger than that between B_{F1} (FBM) and B_{F1} (FBM) by equation (14). That means the stability of the SBM is better and so the SBM is selected and developed for the theoretical bending model of the bending evaluation system of fabric and yarn.

Table 3 The correlation coefficients of the bending rigidity by BES-FY, KES-FB2 and FAST-2.

	B_{F1} (SBM) by equation (14)	B_{F1} (FBM) by equation (14)	B_{F1} (SBM)	B_{F1} (FBM)	B_{F2}	B_{F3}
B_{F1} (SBM) by equation (14)	1					
B_{F1} (FBM) by equation (14)	0.998	1				
B_{F1} (SBM)	0.999	0.996	1			
B_{F1} (FBM)	0.990	0.985	0.991	1		
B_{F2}	0.967	0.968	0.965	0.939	1	
B_{F3}	0.987	0.995	0.983	0.968	0.973	1

Conclusions

Using Timoshenko's elastic theorem, the shifting-point bending model (SBM) and the fixed-point bending model (FBM) were developed, and the deviations of the bending rigidity calculated from both the general and the differential equations were not higher than 0.022, and the two equations can both be used to obtain the bending rigidity; however, the deviation between the SBM and FBM is only 0.08. The experiments conducted by BES-FY show that the bending rigidity of fabric and yarn is best calculated at a curvature range within $1.5\text{--}2.5\text{ cm}^{-1}$. The relationships between bending moment and curvature or between bending rigidity and curvature should be divided into three sections: i.e., quadratic (linear), polynomial of order three (quadratic) and linear (constant) functions. According to the principle of the apparatus developed by the authors, the bending, weight, friction and tensile properties of fabric and yarn can be easily and accurately measured in-situ. Meanwhile, the results of the correlation analysis show that the correlation coefficients of the bending rigidity between the two bending models, i.e., SBM and FBM, and the other measurements, i.e., KES-FB2 and FAST-2, were all better than 0.939, especially for SBM. Therefore, the two bending models can be used to characterize the bending behavior of fabric and yarn and SBM is better than FBM.

Acknowledgment

The authors wish to thank the Textile Materials and Technology Laboratory of Dong Hua University (formerly the China Textile University) for supporting this research.

Literature Cited

- Hearle, J. W. S., Potluri, P., and Thammandra, V. S., Modelling Fabrics Mechanics, *J. Textile Inst.* **92**(3), 53–69 (2001).
- Peirce, F. T., The Geometry of Cloth Structure, *J. Textile Inst.* **28**(3), 45–97 (1937).
- Clapp, T. G., and Peng, H., Buckling of Woven Fabrics, Part III: Experimental Validation of Theoretical Models, *Textile Res. J.* **90**(11), 641–645 (1990).
- Zhou, N. Y., and Ghosh, T. K., On-Line Measurement of Fabric Bending Behavior, Part II: Effects of Fabric Nonlinear Bending Behavior, *Textile Res. J.* **68**(7), 533–542 (1998).
- Leaf, G. A. V., Analytical Plain Weave Fabric Mechanics and the Estimation of Initial Shear Modulus, *J. Textile. Inst.* **92**(3), 70–79 (2001).
- Kawabata, S., “The Standardization and Analysis of Hand Evaluation,” 2nd ed., HESC, The Textile Machinery Society of Japan, Osaka, Japan, 1980.
- Ly, N. G., Tester, D. H., Buckenham, P., Rocznok, A. F., Adriaansen, A. L., Scaysbrook, F., and de Jong, S., Simple Instruments for Quality Control by Finishers and Tailors, *Textile Res. J.* **61**(5), 402 (1991).
- Barndt, H., Fortess, F., Wiener, M., and Furniss, J.C., The Use of KES and FAST Instruments, *Int. J. Cloth. Sci. Technol.* **2**(3/4), 34–39 (1990).
- Grosberg, P., and Swani, N.M., The Mechanical Properties of Woven Fabrics, Part IV: The Determination of the Bending Rigidity and Frictional Restraint in Woven Fabrics, *Textile Res. J.* **36**(4), 338–345 (1966).
- Yu, W.D., and Du, Z.Q., “A New Measurement and Apparatus to Measure Tensile, Compress, Bursting and Piercing Properties of Textile Materials,” China Patent: ZL200410066649. X, 2004.
- Yu, W.D., and Wang, J.C., “The Measuring Equipment of the Bending Rigidity of Yarn,” China Patent: ZL00217564.9, 2001.
- Timoshenko, S., and Gere, J. M., “Theory of Elastic Stability,” McGraw Hill, New York, 1961.
- Kawabata, S., “Textile Structural Composites,” Composite Materials Series 3. University of Delaware, Newark, DE. U.S.A. 1989.
- Grospebr, P., The Mechanical Properties of Woven Fabric, Part II: The Bending of Woven Fabrics, *Textile Res. J.* **36**(3), 205–211 (1966).
- Abbott, G. M., Grosberg, P., and Leaf, G. A. V., The Mechanical Properties of Woven Fabrics, Part VII: The Hysteresis During Bending of Woven Fabrics, *Textile Res. J.* **41**(4), 345–358 (1971).
- Clapp, T. G., and Peng, H., A Comparison of Linear and Non-Linear Bending Models for Predicting Fabric Deformation in Automated Handling, *J. Textile Inst.* **82**(3), 341–352 (1991).
- Owen, J. D., The Bending Behaviour of Plain-Weave Fabrics Woven from Spun Yarns, **59**(3), 313–343 (1968).
- Huang, N. C., Finite Biaxial Extension of Completely Set Plain Woven Fabrics, *J. Appl. Mech.* **46**, 651–655 (1979).
- Livesey, R. G., and Owen, J. D., Cloth Stiffness and Hysteresis in Bending, *J. Textile Inst.* **55** (5), 516–530 (1964).
- Kang, T.J., Joo, K.H., and Lee, K.W., Analyzing Fabric Buckling Based on Nonlinear Bending Properties, *Textile Res. J.* **74**(2), 172–177 (2004).
- Wei, M., and Chen, R.J., The Theory of the Resistance to Bending of Set Plain-Woven Fabrics, *J. Textile Inst.* **85**(3), 359–375 (1994).
- Zhou, N. Y., and Ghosh, T. K., On-Line Measurement of Fabric Bending Behavior, Part II: Dynamic Considerations and Experimental Implementation, *Textile Res. J.* **69**(3), 176–184 (1999).